ELSEVIER

PII: S0032-3861(97)10382-2

Polymer Vol. 39 No. 16, pp. 3827–3833, 1998

0032-3861/98/$19.00+0.00

SAXS study on poly(dimethylsiloxane) networks with controlled distributions of chain lengths between crosslinks

Kenji Urayama*, Takanobu Kawamura, Yoshitaka Hirata and Shinzo Kohjiya
Institute for Chemical Research, Kyoto University, Uji, Kyoto-fu 611, Japan
(Received 30 October 1997; revised 27 November 1997; accepted 4 December 1997)

Supermolecular structures for poly(dimethylsiloxane) (PDMS) gels with unimodal and bimodal distributions of the chain lengths between the crosslinks are investigated by a small angle X-ray scattering (SAXS) technique. The unimodal and bimodal networks are prepared by the end-linking reaction of oligomeric and polymeric dimethylsiloxane mixtures with a series of compositions, and they are fully swollen in toluene. The scattering profiles for unimodal networks primarily depend on whether the precursor chains are highly entangled or not in the uncrosslinked state. For bimodal networks, the correlation lengths Ξ for the supermolecular structures do not strongly depend on the mixing ratio of the precursor chains, and the values are close to Ξ for the unimodal network of oligomeric chains. The value of Ξ for the unimodal network of polymeric chains is larger than for the unimodal network of oligomeric chains, while it is considerably reduced by adding a small amount of the oligomeric chain. The experimental results are interpreted on the basis of the shortest closed circuits concept describing spatial non-uniformities formed by end-linking, and the consideration that the elementary meshes in the networks composed of long precursor chains are mainly formed by entanglements.

(Keywords: SAXS; polymer networks; polymer gels)

INTRODUCTION

The structure of polymer gels has attracted the attention of physicists and physical chemists as an interesting example of amorphous structures. It was often considered that the structure of polymer gel is analogous to that of polymer solution, since the polymer gel is a three-dimensional polymer network containing solvent. A significant difference between them is that gel has a connectivity of polymer chains due to crosslinks. Recently, it has been reported that small angle X-ray or neutron scatterings (SAXS or SANS) of swollen polymer networks exhibit some features which cannot be explained by the classical concept: an excess scattering of polymer gels relative to the solutions with identical polymer concentration; an abnormal butterfly pattern of uniaxially stretched gels[1]. Two independent concepts have been proposed for the origin of these phenomena: one is a spatial inhomogeneity frozen in crosslinked network[2–7], and the other is a coupling between strain and thermal concentration fluctuation[8]. The recent analysis of the static speckle patterns, which are obtained by scanning through various positions in a gel with a laser beam, indicates that the primary origin of the phenomena is attributable to an inhomogeneity quenched in the crosslinked networks[9–11]. These studies clearly indicate that polymer gels have a certain long-range spatial heterogeneity which does not exist in polymer solution. However, the type of quenched inhomogeneity depends on the kind of network system, and some models representing the quenched inhomogeneities have been proposed together with the corresponding scattering functions[1–7]. The spatial inhomogeneities in randomly crosslinked networks, which are made by introducing the crosslinks randomly into long precursor chains, have been explained in terms of the non-uniform distribution of the crosslinks leading to the formation of regions with different crosslinking density.

It has been known that end-linked networks, which are prepared by the end-linking reaction of the precursor chains with a definite molecular weight, in the swollen state also exhibit an excess scattering of qualitatively the same type as for randomly crosslinked networks[4,11,12]. The concept of the non-uniform distribution of crosslinks employed for randomly crosslinked networks is not directly applicable to end-linked networks. Another type of spatial inhomogeneity different from randomly crosslinked networks should be considered, but it has remained unclear[4]. Recently, a concept has been proposed to describe the spatial non-uniformities formed by end-linking[1,11]. The model attributes the non-uniformities to 'shortest closed circuits' with various sizes originating from the fluctuation in connectivity. The concept of the shortest closed circuits suggests the possibility that even if all the precursor chains have the same size and the reaction of all the functional groups in the system is achieved, the resulting network has a long-range spatial inhomogeneity.

The network structure in the short-scale concerning the network chain length (i.e. mesh size) also remains inconclusive. There have been two different standpoints on the determinant of an elementary mesh of swollen networks: one is based on the 'original' c^* theorem[13] postulating the complete disinterpenetration (i.e. no overlapping) of precursor chains at equilibrium swelling[12,14]. It regards a single precursor chain itself as an elementary mesh of end-linked networks. The other considers that some

* To whom correspondence should be addressed

Table 1 Number-, weight- and viscosity-average molecular weights (M_n, M_w and M_η, respectively) of precursor PDMS chains

	M_n	M_w	M_η	M_w/M_n
PS	4.24×10^3	6.81×10^3	4.44×10^3	1.61
PM	2.00×10^4	3.79×10^4	3.61×10^4	1.90
PL	4.61×10^4	7.98×10^4	7.48×10^4	1.73

Table 2 Number-average molecular weights of precursor chains (M_{av}), polymer volume fractions in equilibrium swollen state (ϕ_e), correlation lengths for supermolecular structures (Ξ) for unimodal and bimodal network samples

Sample	mol% of short chains	M_{av}	ϕ_e	Ξ (Å)
US	100	4.24×10^3	0.251	56.6
UM	0	2.00×10^4	0.100	100
UL	0	4.61×10^4	0.0793	107
B91	0.900	8.43×10^3	0.157	66.3
B82	0.800	1.26×10^4	0.170	64.4
B64	0.600	2.10×10^4	0.135	64.8
B37	0.300	3.35×10^4	0.164	60.0
B19	0.100	4.19×10^4	0.143	59.2

degree of overlapping of precursor chains exists in the fully swollen state, and that the elementary meshes are governed by entanglement couplings trapped in the networks, termed trapped entanglements[15–20]. Strictly, there is a significant difference between Refs [15–20] that Ref. [15] is based on the 'modified' c^* theorem where the trapped entanglements are treated as elastically effective crosslinks, while Refs [16–20] have argued the affine displacement of crosslinks in swelling. The problem about the determinant of the elementary mesh of swollen networks has been discussed mainly from the viewpoint of the degree of equilibrium swelling and elastic modulus for end-linked networks. Although SAXS and SANS measurements of swollen networks concentrate on the elucidation of a long-range spatial heterogeneity in the structures, they may also give some significant information about the short-range structure concerning the elementary mesh.

A significant merit of the end-linking methods is that they enable us to prepare networks in which the distributions of the distances between crosslinks are controlled. Soni and Stein[21] prepared networks with the unimodal and bimodal distributions of the chain lengths between crosslinks by end-linking the mixtures of the long and short chains with various mixing ratios, and investigated the light scatterings of these networks. It is naturally expected that the bimodal networks are more inhomogeneous in the scale of mesh size than the unimodal networks. However, their experimental results suggest that the situation in a larger spatial scale is not so simple. In their study[21], the excess scatterings in the small q (1.1×10^{-3} Å$^{-1} < q < 2.3 \times 10^{-3}$ Å^{-1} where q is the scattering vector) varied with the content of short precursor chains in a complicated manner: the excess scattering for the bimodal network with 95 mol% short chains was larger than for the unimodal network of the short chains, but it was smaller than for the unimodal one of the long chains; the excess scattering is maximum for the bimodal one with 50 mol% short chains, although the polymer volume fraction is maximum for the unimodal one of the short chains. This complicated but interesting dependence of the excess scattering on the mixing ratio has not yet been elucidated even qualitatively.

In this study, we have investigated the SAXS of the swollen unimodal and bimodal networks prepared by end-linking the mixtures of polymeric and oligomeric dimethylsiloxane chains with a variety of mixing ratios. The size ratio of the long chains to the short ones by number-average molecular weight was *ca*. 11. The dependence of the SAXS profiles for the unimodal networks on the size of the precursor chains has been investigated. The scattering patterns for the bimodal networks have been examined as a function of the mixing ratio. The experimental results have been interpreted on the basis of the shortest closed circuits concept together with the consideration that elementary meshes in the networks composed of polymeric precursor chains are governed by trapped entanglements.

EXPERIMENTAL

Samples

Three kinds of poly(dimethylsiloxane) (PDMS) differing in average molecular weight, designated as PS, PM and PL, were employed as the precursor chains for end-linking. PS and the others have the methacryloyl (CH_2=C(CH_3)COO) and vinyl groups at both ends, respectively. The number-average and weight-average molecular weight (M_n and M_w, respectively) of each precursor chain were determined by gel permeation chromatography (GPC). The chromatograms were obtained with a Shimadzu GPC LC-6A equipped with a Shim-pack GPC80MC column. Polymer concentration of the elutes was detected by differential refractive analysis. The GPC measurements were made at 54°C using chloroform as solvent under a flow rate of 1.0 ml min^{-1}. Under these conditions, the molecular weight of PDMS is directly obtained from a calibration curve of a series of standard polystyrenes without any further calculations[22]. The viscosity-average molecular weight (M_η) for each precursor chain was obtained from intrinsic viscosity ($[\eta]$) in toluene on the basis of the $[\eta]$–M relationship for the oligomeric[23] or polymeric[24] dimethylsiloxane/toluene system. The values of M_n, M_w and M_η for each precursor chain are listed in *Table 1*.

Tetrakisdimethylsiloxysilane was used as a crosslinker. The end-linking reaction was performed by hydrosilylation at 100°C for 24 h using the Spier's catalyst ($H_2PtCl_6 \cdot 6H_2O$). Three kinds of unimodal networks were made by end-linking PS, PM and PL, which are designated US, UM and UL, respectively. A bimodal network was prepared by end-linking a mixture of PS and PL with a certain molar mixing ratio. The molar mixing ratios of PS to PL by M_n were 1/9, 3/7, 6/4, 8/2 and 9/1. The corresponding bimodal networks are designated as B19, B37, B64, B82 and B91, respectively. The average molecular weight (M_{av}) of a mixture of the precursor chains for each sample is shown in *Table 2*. The molar ratio of the functional groups in the precursor chains to [SiH] groups in the crosslinkers was stoichiometric in the preparation of all the network samples.

The network samples were immersed in toluene until equilibrium swelling was achieved. Unreacted materials were thoroughly washed out by renewing the toluene every day. The polymer volume fraction in equilibrium swollen networks (ϕ_e) was determined by measuring the weights of the samples in the equilibrium swollen and fully dry state together with the assumption of the additivity with respect to volume. The fully dry state was achieved by drying the swollen gels in which the unreacted materials had been extracted. The values of ϕ_e for each sample are listed in

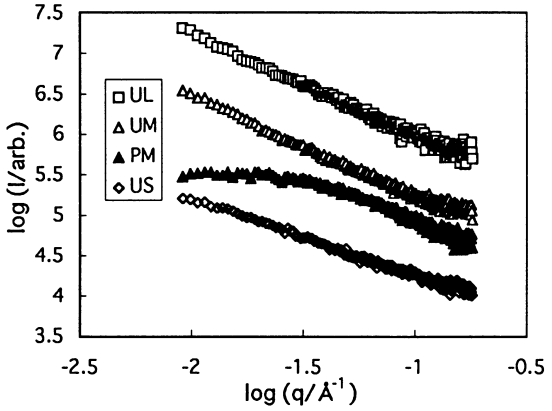

Figure 1 SAXS profiles for the unimodal networks and the PM solution with $\phi = 0.1$. The curves for the networks are arbitrarily shifted in the vertical direction to prevent them from overlapping

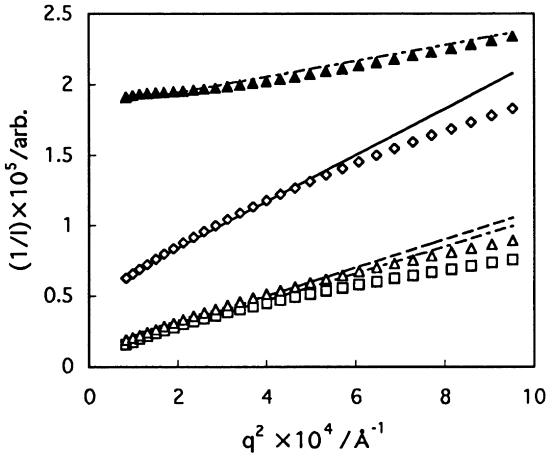

Figure 2 Plots of the inverse of I against q^2 for the unimodal networks and PM solution with $\phi = 0.1$ (symbols as in *Figure 1*)

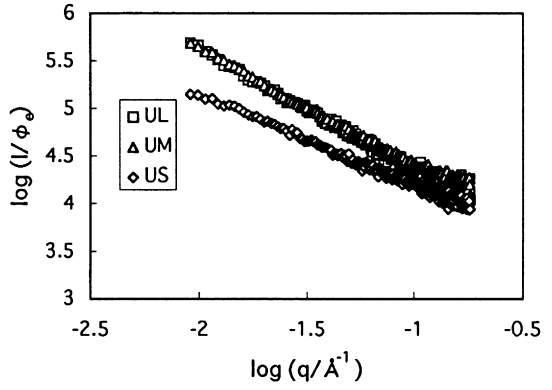

Figure 3 Normalized SAXS profiles for the unimodal networks

Table 2. The weight fractions of the unreacted materials for all the bimodal network samples were less than 10 wt%. A simple calculation shows that the quantities of the unreacted materials are not so large as to cause significant differences in the compositions of the precursor chains before and after crosslinking, i.e. the mixing ratios in the preparation were realized in the resulting networks with an accuracy enough not to prevent quantitative discussion.

SAXS measurements

SAXS measurements were performed with an SAXES optics[25] installed at BL-10C of the Photon Factory of National Laboratory for High Energy Physics, Tsukuba, Japan. The wavelength of the incident X-ray from synchrotron radiation was 1.488 Å. Samples were placed in a cell having two mica windows separated by 2 mm. The scattered X-ray was detected by a one-dimensional position-selective proportional counter (PSPC). The calibration for the sensitivity to X-ray at each position of PSPC was carried out. A toluene sample was used for background subtraction. The contribution of the empty cell was also subtracted.

RESULTS

Unimodal networks

Figure 1 shows the SAXS profiles of the unimodal networks UL, UM and US in the equilibrium swollen state. The SAXS profile for the PM solution with $\phi = 0.1$ equal to ϕ_e of UM is also shown. The profiles for the networks are arbitrarily shifted in the vertical direction to prevent them from overlapping. As is clearly seen, the scattering intensities (I) in the small q region for UM are much larger than for the PM solution. The excess scatterings of this type are substantially similar to those reported for various swollen gels[1]. It is also seen that the values of I for UL and UM are not fully saturated in the low q limit, while the q dependence of I for US shows the quasi-plateau in the small q region. A definite level off of I for UL and UM presumably occurs at a lower q.

Figure 2 shows the plots of the inverse of I *versus* q^2 in $q < 3.1 \times 10^{-2}$ Å^{-1} for PM solution and the unimodal networks. It can be seen that the data points for PM solution, and in $q < 2.3 \times 10^{-2}$ Å^{-1} for the unimodal networks fall on the straight lines. The scattering spectra which show the linear relation between I and q^2 are satisfactorily described by the following Ornstein–Zernike function[1]:

$$I(q) = \frac{I(0)}{1 + q^2\Xi^2}. \quad (1)$$

Here, Ξ is the correlation length, and values of Ξ obtained for the network samples are given in *Table 2*. It is seen that the values of Ξ for UL and UM are comparable, while those for US are larger. The value of the correlation length ξ obtained for PM solution was 17.7 Å which agrees well with $\xi = 17.5$ Å from the experimental relation ($\log \xi = 0.504 - 0.74 \log \phi$) for the PDMS–toluene solution reported by Mallam *et al.*[26]. M_η ($= 4.0 \times 10^4$) of PDMS used in their SANS study is almost the same as that of PM ($= 3.6 \times 10^4$). Here, we assigned ξ and Ξ to the correlation lengths for polymer solution and gels, respectively, because they have different physical origins: ξ and Ξ are related to the dynamic fluctuation of polymer concentration and the static frozen heterogeneities in the gels, respectively.

In a sufficiently high q region, the q dependence of I is expected to approach asymptotically to one for an isolated polymer chain with excluded volume effect, i.e. $I \sim q^{-D}$ with $D \cong 5/3$ where D is the fractal dimension[1]. However, the q dependence of I in high q in *Figure 1* is not so strong as the expected power law, indicating that the high q limit in this study does not reach the q region showing the spatial correlation characteristic of a single network chain.

Figure 3 indicates the reduced scattering profiles for the unimodal networks after the conventional normalizing

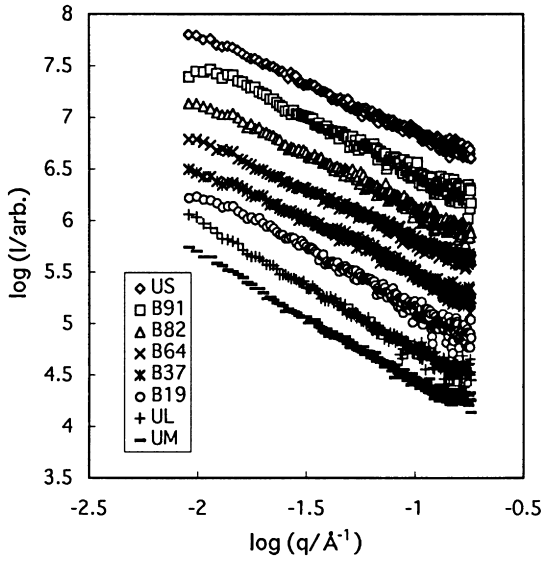

Figure 4 SAXS profiles for the bimodal networks together with the unimodal networks. The curves are arbitrarily shifted in the vertical direction to prevent them from overlapping

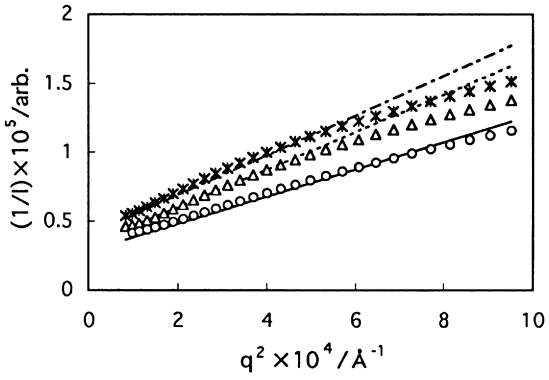

Figure 5 Plots of the inverse of I against q^2 for B82, B64 and B37 (symbols as in *Figure 4*)

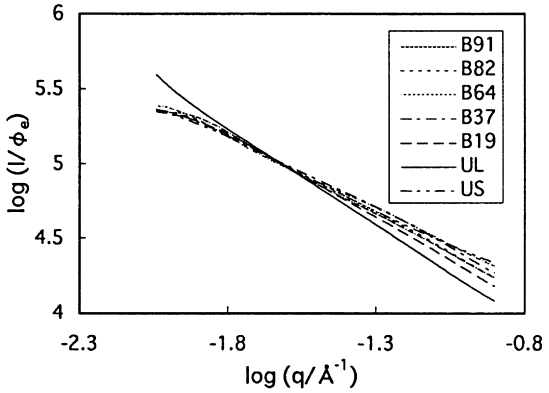

Figure 6 Normalized SAXS profiles for the bimodal networks, US and UL

method, i.e. the normalization of I by ϕ_e[1]. In the normalization procedure, we took the magnitudes of the influences of experimental errors on the normalization into account. The results of the normalization are influenced by the experimental errors involved in the determination of the film thickness and ϕ_e, the magnitudes of which were evaluated to be *ca*. 10% and *ca*. 2%, respectively. The vertical shift caused by these experimental errors is $\pm$ 0.02 decade. It is found in *Figure 3* that the q dependence of I for US is weaker than for UL and UM, while the profiles for UL and UM coincide over the whole q.

Bimodal networks

Figure 4 shows the SAXS profiles for a series of bimodal networks in the fully swollen state together with those for the unimodal networks. The profiles are vertically shifted to an arbitrary degree to avoid overlapping. The quasi-plateau of $I(q)$ in the low q region is observed for all the bimodal networks. It should be noted that the quasi-plateau in small q, which is not observed in UL, appears in B19 in spite of the small fraction (10 mol%) of PS. It is also found that the scattering profiles for the bimodal networks show a shoulder at $q \cong 2.5 \times 10^{-2}$ Å^{-1}, although it is not very enhanced. The shoulder is especially noticeable for B91 and B82. The effects of the bimodal size distributions of precursor chains on the network structures are clearly found in the comparison of the curves for B64 and UM which were prepared by the precursor chains with almost the same average molecular weights. The $I(q)$ for B64 shows the level off at small q and the shoulder aspect both of which are not seen for UM.

Figure 5 shows the plots of I^{-1} *versus* q^2 for B82, B37 and B19. As can be seen, the relations between I^{-1} *versus* q^2 at $q < 2.5 \times 10^{-2}$ Å^{-1} are well expressed by the straight lines. The same types of plot using the data for B91 and B64 showed a similar behaviour, though the data are not shown in the figure. As mentioned before, these results mean that the scattering spectra in $q < 2.5 \times 10^{-2}$ Å^{-1} for the bimodal networks are well reproduced by equation (1). We show in *Table 2* the values of Ξ for the bimodal networks. The experimental error in Ξ is estimated to be $\pm$ 3 Å. The values of Ξ for the bimodal networks do not seem to depend strongly on the mixing ratio.

It can be seen that the q dependence of I in the high q region is influenced by the mixing ratio, and it tends to become stronger with the increase in the PL fraction.

Various types of scattering functions have been proposed to reproduce the scattering spectra over the entire q for polymer gels[1]. They are roughly divided into two groups, one of which is a generalized Ornstein–Zernike function[27], and the other is a combination of two different functions: a Lorentzian and squared Lorentzian[5]; a Lorentzian and Gaussian[2]; a Lorentzian and stretched exponential[28]; another two complex functions[6]. It should be noted that none of them satisfactorily and consistently reproduce the present experimental scattering patterns over the whole q for all the networks in this study.

In order to compare closely the SAXS profiles for a series of bimodal networks, we show in *Figure 6* the normalized ones in which I were reduced by ϕ_e. The curves were obtained by smoothing the normalized data by the polynomial functions so that the profiles of different samples can be clearly discriminated. It is found that the reduced scattering spectra for a series of bimodal networks and US agree well in the low q region ($q < 4 \times 10^{-2}$ Å^{-1}), while they are separated in the high q region.

DISCUSSION

Unimodal networks

The excess scatterings of UM relative to PM at small q in *Figure 1* suggest the existence of some supermolecular

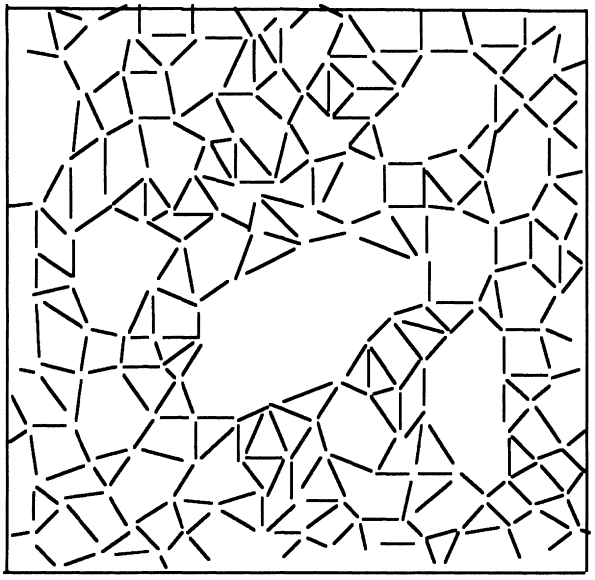

Figure 7 Schematic representation of the supermolecular structure in an end-linked network on the basis of the shortest closed circuits concept[1,11]. The functionality of crosslink is four

structure with a large correlation length in the network. The supermolecular structures formed by end-linking are likely to be qualitatively explained by the concept of the shortest closed circuits (SCCs)[1,11]. The SCC concept attributes the long-range spatial inhomogeneities to the size distribution of the SCCs resulting from the fluctuation of connectivity. An example of supermolecular structures based on the SCC concept is schematically shown in *Figure 7* where the functionality of crosslinks (f) is four. *Figure 7* well represents a topological feature of an end-linked network system: a fluctuation of connectivity resulting in a long-range spatial inhomogeneity emerges in the network, even if all the functional groups have reacted. In an actual reaction bath, it is difficult to conduct the reaction fully quantitatively, i.e. the complete reaction of all the functional groups. This is mainly due to the increase of steric hindrance around the functional groups during the crosslinking reaction[29–31]. The incompleteness in the reaction generates crosslinks whose functionality is less than four, i.e. three, two or even one, which leads to a further increase in the fluctuation of connectivity[29–32]. The supermolecular structure consists of two regions differing in the density of network chains: the region in which the precursor chains are connected to each other; the region which is empty of precursor chains (corresponding to shortest closed circuit). This type of supermolecular structure may be common to many unimodal networks prepared by end-linking, while the correlation length for a supermolecular structure (Ξ) should depend on the size of the precursor chain. Ξ corresponds to the mean size of the SCCs which is roughly equivalent to the inter-cluster distance. Here, 'cluster' means the region in which the density of network chains is higher than the average.

It is expected from *Figure 7* that the supermolecular structures based on the SCC concept possess a fractal nature: when the elementary mesh size becomes larger, Ξ increases in proportion to the elementary mesh size, while the q dependence of I is unchanged, i.e. the scattering curve is shifted to the smaller q side keeping the identical shape. On the basis of this concept, the larger values of Ξ for UM and UL than for US are attributable to the larger molecular masses of PM and PL than of PS. On the other hand, UM and UL had comparable values of Ξ, and both the reduced scattering profiles showed the almost perfect coincidence over the whole q without any horizontal shift, in spite of the considerable size difference between PM and PL. These results strongly suggest that the elementary meshes in UM and UL are governed not by the chemical crosslinks but by trapped entanglements. The molecular weight between adjacent entanglements (M_e) and the critical molecular weight for the formation of entanglement couplings (M_c) were reported to be 8.1×10^3 (Ref. [33]) and 1.66×10^4 (Ref. [34]) for PDMS, respectively. The molecular weight of PS is smaller than M_e, while those of PM and PL are larger than M_c. This also suggests the consideration that the elementary meshes in US are primarily governed by PS, while those in UM and UL are determined by trapped entanglements. (Our previous study[20] on the elastic modulus of end-linked PDMS networks suggested that even if the molecular mass of the precursor chain is less than M_c, a certain amount of trapped entanglements are formed. However, in such a network, the chemical crosslinks are major in quantity, while the trapped entanglements are minor.) In addition, values of ϕ_e for UM and UL are comparable, so that UM and UL have an elementary mesh with almost the same size, and show quite similar spatial correlations over the whole q.

The almost perfect coincidence of the reduced scattering curves without any horizontal shifts, and the comparable values of Ξ for UM and UL strongly suggests that the complete disinterpenetration of precursor chains in the fully swollen state, which the original c^* theorem postulates, does not occur. According to the postulate of the original c^* theorem, a finite horizontal shift must be necessary for the superposition of the reduced scattering curves, and a significant difference in Ξ should be observed for UM and UL. The magnitude of the horizontal shift and the ratio of Ξ for UM and UL may be given by the ratio of the dimension of PM and PL in good solvent, i.e. $(M_{PL}/M_{PM})^{0.6}$ where M_{PL} and M_{PM} are the molecular mass of PL and PM, respectively. The ratio is estimated to be *ca.* 1.6, which corresponds to 0.2 decade as horizontal shift factor. Such a difference is not observed in Ξ and the scattering curves for UL and UM. The invalidity of the postulate of the original c^* theorem has also been reported in some swelling experiments[15,18–20].

From a strict viewpoint of the fractal nature of the SCC concept, the normalized scattering curve for US is requested to have the same shape as those for UM and UL, and to be located at the larger q side relative to those for UM and UL according to the difference in the elementary mesh sizes (i.e. M_e and M_{PS}). However, as is seen in *Figure 3*, the q dependence of I over the whole q for US is slightly weaker than for UM and UL, implying that the spatial correlation for supermolecular structure in US is not entirely identical with those in UM and UL. This discrepancy may originate from some differences in the details of the supermolecular structure between the two kinds of network whose elementary meshes are governed by entanglement couplings and by the oligomeric precursor chains themselves. We consider that the supermolecular structures in both the network systems are essentially described by the SCC concept, although some differences in the details of the supermolecular structures between them are observed.

Bimodal networks

The agreement in the reduced spectra at small q for a series of bimodal networks and US, which is seen in

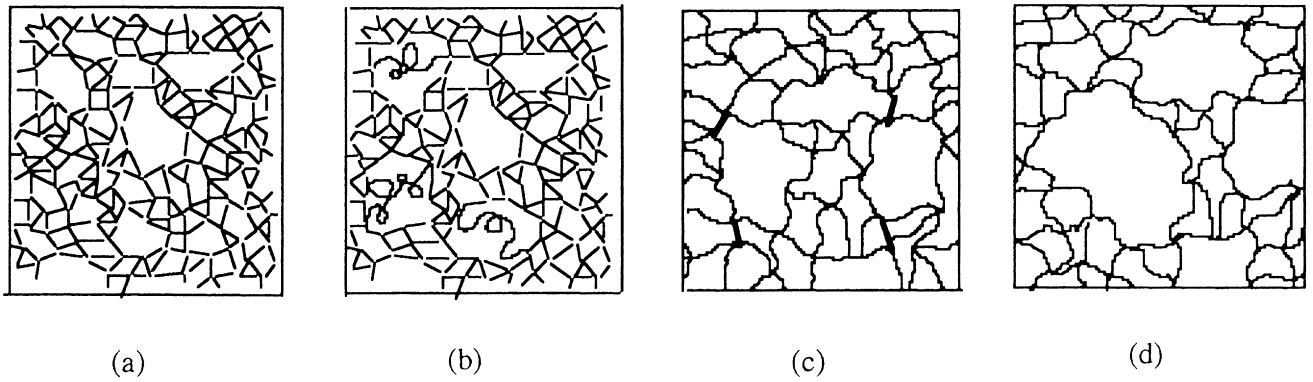

Figure 8 Schematic representation of supermolecular structures in bimodal networks with a series of PS fractions: (a) with 100 mol% PS; (b) with a large PS fraction; (c) with a small PS fraction; (d) with 0 mol% PS. The elementary mesh size in (a) is equivalent to the size of PS, while that in (d) corresponds to the distance between adjacent trapped entanglements

Figure 6, means that the spatial correlations for the supermolecular structures in these networks are similar. This is also shown by the fact that Ξ for the bimodal networks does not strongly depend on the mixing ratio, and the values are close to those for US. We may approximate $\Xi \cong 60$ Å for the bimodal networks irrespective of the mixing ratio. It is surprising that there are no great differences in the long-range spatial correlations between a series of bimodal networks and US, and that the discrepancies are observed only in the relatively small-range spatial correlations. Furthermore, it is noteworthy that Ξ for UL is considerably decreased by the addition of the small amount of PS, which is clearly demonstrated by the emergence of saturation in I at low q for B19 which is not observed for UL. This result means that the long-range concentration fluctuation in the unimodal network of the long chains is depressed by the addition of a small amount of short chains, which is contrary to the intuitive concept that Ξ for B19 is larger than or comparable to that for UL. We propose a structural model which explains the above experimental results in the next section.

In the high q region, the q dependence of I showed the tendency to become weaker with increasing PS fraction. This should be because the screening effect on the excluded volume effects in the polymeric network chains by the oligomeric ones is enhanced with increasing the PS fraction.

Supermolecular structure in unimodal and bimodal networks

Firstly, we discuss the supermolecular structure in the unimodal networks. As stated in the previous section, the supermolecular structures for the unimodal networks are substantially described by the network structure having SCCs with various sizes. Ξ for the unimodal networks should correspond to the mean size of the SCCs. Since the elementary unit in the SCC concept is the mesh of the network, Ξ primarily depends on the elementary mesh size. Ξ increases with increasing size of the precursor chains (equivalent to the elementary mesh size), as long as the precursor chains are so oligomeric that entanglement couplings are not formed in the uncrosslinked state. When the precursor chains are polymeric enough to be highly entangled before crosslinking (i.e. the mesh size is mainly determined by trapped entanglements), Ξ remains constant (Ξ_L) regardless of the size of the precursor chains. The schematic representation for the supermolecular structures in US and UL are drawn in *Figure 8a* and *d*, respectively. It should be noted that in *Figure 8a* and *d* the elementary mesh sizes correspond to the size of the oligomeric precursor chain itself and the distance between adjacent trapped entanglements, respectively. We expect that the molecular mass of elementary mesh in UL is about twice as large as in US on the basis of the difference between $M_e = 8100$ and the molecular weight of PS.

For the bimodal networks, at first, we consider the system with a large fraction of PL such as sample B19. An important key for the supermolecular structure in such a network is the significant difference in Ξ between UL and B19. Employing the SCC concept together with the recognition that the elementary meshes in UL are governed by trapped entanglements, we semi-quantitatively explain the significant reduction in Ξ for UL by only 10 mol% addition of PS in the following. The change in the structure from UL to B19 may be simply described by the replacement of one PL chain with one PS chain per 10 PL chains in UL. The PL chains in UL have 6–10 entanglement points per chain. The replacement of a PL chain with a PS chain means that 6–10 elementary meshes are lost, and the PS chain, whose size is almost half as long as the entanglement distance, is inserted instead. Here, we roughly estimate the degree of reduction in the mean size of the SCCs caused by such a replacement. Let us consider a circle with diameter 107 Å equal to Ξ for UL. The circumference of this circle corresponds to *ca*. 18 pieces of elementary mesh formed by entanglements. Here, the size of the elementary mesh (ξ) was calculated using $3^{1/2}\xi = \langle R_g^2 \rangle^{1/2} = 0.17M^{0.58}$ (Å)[35] with $M = 8.1 \times 10^3$ where $\langle R_g^2 \rangle$ is the mean-square radius of gyration. For simplicity, if the replacement is entirely applied to the circumference (i.e. a whole PL chain is a part of the circumference), *ca*. 8 pieces of elementary mesh on the circumference are lost by the replacement. Consequently, the diameter of the circle is decreased to *ca*. 60 Å. (Here, the contribution of the inserted PS chain to the reduced circumference was neglected for simplicity.) Though this estimation is primitive, it at least semi-quantitatively explains the significant difference in Ξ between UL and B19. It should be emphasized that if an elementary mesh is assumed to correspond to a PL chain, which is the postulate of the original c^* theorem, the degree of reduction in the diameter of the circle by such a replacement remains not more than 20%, which is too small to explain the experimental results.

Almost the same value of Ξ for B19 and B37 would suggest that the reducing effects on Ξ by the addition of PS are saturated at a PS fraction of less than 10 mol%. It is also interesting that the values of Ξ for B19 and B37 are almost

equal to that for US. This indicates that the mean size of the SCCs reduced by the addition of PS (Ξ_{LS}) is comparable to that for the unimodal network of PS (Ξ_S) (i.e. $\Xi_{LS} \cong \Xi_S$), as is shown in *Figure 8*.

Next we consider the bimodal networks with a large fraction of PS such as samples B91 and B82. The experimental results showed that Ξ for US is close to that for B91 and B82. However, the types of supermolecular structures in US and B91 should be different. The network structure for B91 and B82 has two regions very different in hardness, one of which is composed of a number of PS chains, and the other contains a PL chain. Swelling will have the effect of clarifying such a heterogenity in the network structures: the soft regions swell more than the hard ones, so that a PL chain is disinterpenetrated. The situation is schematically shown in *Figure 8b*. If Ξ for B91 and B82 corresponds to the distance between the hard domains which is almost equivalent to the size of the soft domains, Ξ will be close to the dimension of a PL chain in an isolated state in good solvent (Ξ_i). It should be noted that Ξ_i ($\cong 69$ Å) is close to Ξ_S. Here, Ξ_i was obtained using the above-mentioned relation between $\langle R_g^2 \rangle$ and M together with $M_w = 7.98 \times 10^4$.

The above considerations explain the experimental results that a long-range spatial correlation is not very sensitive to the mixing ratio except that the difference in Ξ between UL and B19 is significant: as the PS fraction increases from zero to one, the correlation length Ξ for the supermolecular structure will shift continuously in such a way as $\Xi_L \rightarrow \Xi_{LS} \rightarrow \Xi_i \rightarrow \Xi_S$. However, three ($\Xi_{LS}$, Ξ_i and Ξ_S) of the four kinds of Ξ which characterize four different types of supermolecular structure, are unexpectedly comparable (*ca*. 60~70 Å), hence the long-range spatial correlations for US and a series of bimodal networks are almost identical. On the other hand, since the replacement of PL with PS in UL has significantly reduced the mean size of the SCCs even if the PS amount is small, a considerable difference in Ξ_L and Ξ_{LS} is observed. The addition of 10 mol% PS reduces the mean size of the SCCs to a value close to Ξ_i (and Ξ_S), so that any great differences in the long-range spatial correlation are not seen for the networks with PS fractions of more than 10 mol%.

The maximum dependence of the excess scattering on the mixing ratio, which was reported by Soni and Stein[21], has not been observed in this study. In their study, the oligomeric dimethylsiloxane chains whose M_n is 7.7×10^2 was employed, and the size ratio of the long precursor chain to the short one by M_n was *ca*. 29. The oligomeric chain in their study is shorter, and the size ratio is larger than in this study. The significant differences in the experimental results between both studies suggest that the supermolecular structures in the bimodal networks will depend not only on the mixing ratio but also on the molecular mass of the short precursor chain and/or the size ratio of the two kinds of precursor chain. In order to elucidate the dependence of supermolecular structures on these factors, the bimodal networks prepared by controlling these factors systematically should be investigated. This will be the subject of future work.

ACKNOWLEDGEMENTS

The authors are indebted to Prof. K. Kajiwara and Dr H. Urakawa, Kyoto Institute of Technology, for the SAXS measurements and valuable discussions. This work was performed with the approval of the Photon Factory of the National Laboratory for High Energy Physics, Tsukuba, Japan (Proposal No. 95G130). This work is partly supported by a Grant-in-Aid from the Ministry of Education, Science, and Culture of Japan (No. 09750990).

REFERENCES

1. For a review, see, Bastide, J. and Candau, S. J., in *Physical Properties of Polymeric Gels*, ed. A. Cohen. Wiley, New York, 1996, and references cited therein.
2. Hecht, A. M., Duplessix, R. and Geissler, E., *Macromolecules*, 1985, **18**, 2167.
3. Daoud, M. and Leibler, L., *Macromolecules*, 1988, **21**, 1497.
4. Bastide, J., Boue, F. and Buzier, M., in *Polymer Motions in Dense Systems*, eds. D. Richter and T. Springer. Springer-Verlag, Berlin, 1988.
5. Onuki, A., *J. Phys. II France*, 1992, **2**, 45.
6. Falcao, A. N., Pedersen, S. and Mortensen, K., *Macromolecules*, 1993, **26**, 5350.
7. Panyukov, S. and Rabin, Y., *Macromolecules*, 1996, **29**, 7960.
8. Rabin, Y. and Bruinsma, R., *Europhys. Lett.*, 1992, **20**, 79.
9. Joosten, J. G. H., McCarthy, J. L. and Pusey, P. N., *Macromolecules*, 1991, **24**, 6690.
10. Rouf, C., Bastide, J., Pujol, J. M., Schosseler, F. and Munch, J. P., *Phys. Rev. Lett.*, 1994, **73**, 830.
11. Rouf, C., Munch, J. P., Beinert, G., Isel, F., Pouchelon, A., Palierne, J. F., Boue, F. and Bastide, J., *Polym. Gels and Networks*, 1996, **4**, 435.
12. Shibayama, M., Takahashi, H. and Nomura, S., *Macromolecules*, 1995, **28**, 6860.
13. de Gennes, P.-G., *Scaling Concepts in Polymer Physics*. Cornell University Press, Ithaca, New York, 1979.
14. Oikawa, H. and Murakami, K., *Rubber Chem. Technol.*, 1987, **60**, 579.
15. Candau, S., Peters, A. and Herz, J., *Polymer*, 1981, **22**, 1504.
16. Panyukhov, S. V., *Sov. Phys. JETP*, 1990, **71**, 372.
17. Obukhov, S. P., Rubinstein, M. and Colby, R. H., *Macromolecules*, 1994, **27**, 3191.
18. Patel, S. K., Malone, S., Cohen, C., Gillmore, J. R. and Colby, R. H., *Macromolecules*, 1992, **25**, 5241.
19. Urayama, K. and Kohjiya, S., *J. Chem. Phys.*, 1996, **104**, 3352.
20. Urayama, K., Kawamura, T. and Kohjiya, S., *J. Chem. Phys.*, 1996, **105**, 4833.
21. Soni, V. K. and Stein, R. S., *Macromolecules*, 1990, **23**, 5257.
22. Wang, B. and Krause, S., *Macromolecules*, 1987, **20**, 2201.
23. Bianchi, U., Dalpiaz, M. and Patrone, E., *Makromol. Chem.*, 1964, **80**, 112.
24. Haug, V. A. and Meyerhoff, G., *Makromol. Chem.*, 1962, **53**, 91.
25. Ando, T., Yamanaka, S., Kohjiya, S. and Kajiwara, K., *Polym. Gels and Networks*, 1993, **1**, 45.
26. Mallam, S., Horkay, F., Hecht, A.-M., Rennie, A. R. and Geissler, E., *Macromolecules*, 1991, **24**, 2896.
27. Kajiwara, K., Kohjiya, S., Shibayama, M. and Urakawa, H., in *Polymer Gels*, eds. D. DeRossi *et al*. Plenum Press, New York, 1991.
28. Horkay, F., Hecht, A. M., Mallam, S., Geissler, E. and Rennie, A. R., *Macromolecules*, 1991, **24**, 2896.
29. Kohjiya, S., Takada, Y., Urayama, K., Tezuka, Y. and Kidera, A., *Bull. Chem. Soc. Jpn.*, 1996, **69**, 565.
30. Kidera, A., Higashira, T., Ikeda, Y., Urayama, K. and Kohjiya, S., *Polym. Bull.*, 1997, **38**, 461.
31. Urayama, K., Kohjiya, S., Yamamoto, M., Ikeda, Y. and Kidera, A., *J. Chem. Soc., Faraday Trans.*, 1997, **93**, 3689.
32. Gottlieb, M., Macosko, C. W., Benjamin, G. S., Meyers, K. O. and Merril, E., *Macromolecules*, 1981, **14**, 1039.
33. Ferry, J. D., *Viscoelastic Properties of Polymers*, 3rd edn. Wiley, New York, 1980.
34. Orrah, D. J., Semlyen, J. A. and Ross-Murphy, S. B., *Polymer*, 1988, **29**, 1452.
35. Beltzung, M., Herz, J. and Picot, C., *Macromolecules*, 1983, **16**, 580.